Trade-off of beam shape & size in telescope.

Prepared by: Martin Caldwell

1. Summary.

The question is what size & shape to chose for the beam pattern in each of the SPIRE instruments. The trade-off is between stray-light rejection (requiring the instrument beam to be undersized) and throughput plus spatial resolution (requiring the instrument beam to fill the telescope aperture).

Beam patterns (top-hat & gaussian) at the mirrors are analysed for the case with no undersizing, leading to beam clipping in the telescope. The consequences for spatial resolution (diffraction point spread function PSF) and for background signals (stray-light) are calculated.

The conclusion is that the performance is best for the gaussian beam case (although the throughput question is not included here), and that even in the top-hat case the stray-light levels should be acceptable providing we can accept :

a. A susceptibility to external sources (long-wavelength only) at around 3.2 degrees from line of sight (edge of M2).
b. The potential need to notch the instrument pupil stop to block stray light arriving via the telescope spider.

2. Document scope.

The trade-off considered is between two extremes:

1. To use the standard approach which is under-sizing of the instrument pupil relative to the telescope pupil (Lyot stopping) to block the edge-diffraction arising in the telescope (important as the telescope is relatively hot). This minimises stray-light but also involves loss of throughput (not all of telescope aperture is used), and spatial resolution (increased beam width at the sky).
2. To abandon the under-sizing and allow edge-diffraction to occur, with the opposite effect to 1., i.e. possible increased stray light, but maximised throughput and spatial resolution.

This analysis is to begin to quantify the above effects by calculating the beam patterns in the telescope, as a first step to deciding this trade-off. The stray-light effects within the instruments are not included for now because there the thermal emission levels are lower. The analysis proceeds from the telescope focal plane as a time-reversed propagation (outwards to space).

Two types of far-field beam shape are considered: gaussian beam (from coherent or horn detector) and top-hat beam (from incoherent or bare detector, clipped by cold stop). Of these, the gaussian case is expected to be more tolerant to the inclusion edge-diffraction , due its edge-taper (reduced beam intensity at pupil edge). However it also represents a smaller effective collecting aperture in terms of beam full-width at half-maximum at the spacecraft. The consequence of this for throughput depends on the detector responsivities, and so a comparison of throughput between different beam shapes (i.e. detector types) is outside the scope of this note.

The wavelength of analysis is 0.5mm, near the centre of the phot longest wavelength band, as a representative worst case for diffraction.

3. Diffraction model.

The model used is the ASAP one described previously (ref.1,2). Here the initial beam pattern is generated & is converted to a ray-set for propagation. At each component where clipping occurs (here it is the telescope pupil only), the beam pattern is regenerated, the clipping applied to it, and then it is converted into a new ray-set for onward propagation.

The propagation proceeds outwards (fig.1) so that the final pattern is that on the sky. It can be shown that this 'time-reversed' method is equivalent to that of forward propagation, at least in the case where clipping is occurring only at pupil & field planes. For the gaussian (coherent detector) case the sky beam pattern is equivalent to instrument point spread function (PSF), whereas for the top-hat (incoherent detector) case it does not include the effect of finite detector spatial extent (i.e. in each case a point-like detector is assumed). This feature can be added in later updates by repeated propagation runs over the spatial size of the bare detector (ref.2), when this is known.

As shown in fig.1 the components encounter by the beam moving outwards from the telescope focal plane (field stop) are, in order:

1. Rear face of primary mirror (M1).
2. Secondary mirror (M2) (pupil) & surround (cone of sky + spider).
3. Primary mirror front face & surround (sunshield).
4. Sky.

The central obscuration of the beam, which in this model would occur between steps 3 & 4 is not included in this draft.

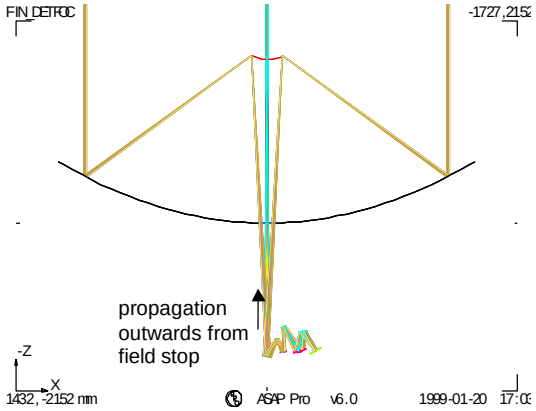

Fig.1. FIRST telescope optical design (bph11.seq).

Of the possible clippings which occur, that at M2 is most important as it applies to all detectors of the array (this is a pupil-plane component), whereas other components will effect mainly the edge-detectors only. Clipping occurring at the rear face of M1 should be relatively small except at the edge of the FOV, as this area can be oversized, and the background should be low because the surround can hopefully be made to reflect back onto the cold area of the instrument. The later clipping at the outside edge of M1 is important as the surround includes the high-emissivity sun-shield.

3.1 Model of the SPIRE instrument beam.

Here the 'beam' we are propagating is that from the centre detector of the FOV.

For beam propagation outward from the detector, the pattern is first considered at the cold stop (instrument System Aperture Stop), where the clipping produces either a top-hat shape (bare detector) or a truncated gaussian shape (horn detector), with a $1/e^2$ edge taper (ref.3). It is assumed this cold stop is in a far-field region of the beam, so that for a detector with perfect phase response the beam has a spherical wavefront shape (no aberrations), with centre-of-curvature at the detector.

On propagating through the instrument various clippings & aberrations may change the beam shape , but these effects are not included here as yet. Consequently the beam pattern from the cold stop is taken to be imaged to the telescope focal plane without aberration. At this point it is clipped by the field stop. This

has the effect of limiting the range of the angular spectrum of plane waves which make up the beam. The diffraction limited resolution for imaging of the beam edge from the instrument pupil to the telescope pupil means that the intensity roll-off at the beam edge is given by the airy function (for circular field stop) with a first dark ring radius of

$$r = 1.22\lambda F \qquad (1)$$

where F is the f-number of the ray bundle which connects the pupils. This is determined by the size of the field stop, and in the telescope it has a value of F= 60 , giving r=35 mm at the telescope pupil. The pupil radius is 137mm (ref.3) so this blurring is a significant fraction of the beam size (hence the desire to avoid having to apply a corresponding undersize of SPIRE's pupil). For other instruments on FIRST operating at longer wavelengths, this blurring may be controlled by using larger field stops than those in SPIRE?

In the present model, since the instrument is not included an alternative way of generating the instrument beam must be used. In the present model it is most convenient to use the sampling of a top-hat function with ASAP's array of gaussian modes, and chosing the sampling resolution to give the correct edge blurring as per equation (1). This method is described in Appendix. 1, and the resulting pattern is shown in fig. 2a, where the edge roll-off (peak-to-zero distance) is 45mm, approx. in line with that given by (1) above, and where the undersizing of the SPIRE pupil is taken to be zero (instrument beam size fills telescope aperture). The ripple seen on the beam in (a) is due to the coarseness of the gaussian mode sampling used in this case (App.1). To improve accuracy this input beam could alternatively be generated synthetically as an amplitude-phase pattern using e.g. IDL , and then converted into rays.

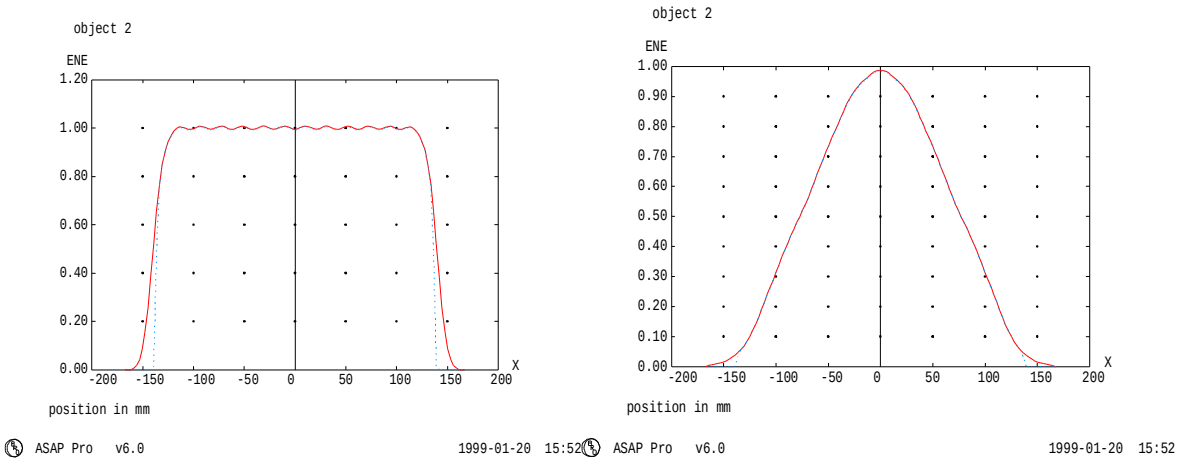

(a) (b)

Figure 2. Cross-section of beam (intensity) patterns at M2, solid line= incident beam, dotted= reflected (clipped). (a) Top-hat case (b) Gaussian case. Radius of M2 is 137mm.

This beam pattern does not include the instrument-induced effects of:

1. Imaging aberrations, which could be added to the M2 beam as wavefront (phase) deformations.
2. Pupil aberrations, which could be added as further smearing of the beam edge. However the degree of pupil aberration is expected to be a few percent, much less than that of the diffraction shown above.
3. Beam clipping at non-pupil plan instrument components. This can only be added by performing the propagation analysis through the complete instrument. Such clipping also changes the aberrations 1.

And 2. Above, so in this case the aberrations must also be modelled via the propagation method, leading to a fully propagation-based model.

Beam patterns.

Figure 2a also shows plots of the beam patterns after clipping by the edge of M2 is applied. In the top-hat case this occurs at approx. the 50% point (since SPIRE pupil undersize = zero), and in the gaussian case at approx 0.5x 1/e^2 = 6.7%. The outer portion which misses M2 will continue outwards into space (assuming M2 has no surround apart from the spider). The stray-light background levels are detailed later.

Figure 3 shows plots of the beam patterns at M1. It can be seen that the clipping by M2 (dotted plot) has the effect at M1 of curtailing the beam edges more sharply than in the case without clipping , as well as adding some ripple near the beam edge. This effect is desirable since on one side of M1 its surround is the hot sunshield, i.e. it is better to clip at M2 than at M1. One reason why the edge-diffraction from M2 is so sharply confined is that the beam at M1 is relatively large in terms of wavelengths(3metres/0.5mm = 6000λ). If the clipping by M1 were to be applied, it would occur somewhat outside the 50% point of the unclipped top-hat beam (solid line) , because the edge of M1 is oversized with respect to the beam according to the telescope FOV. (Its radius in this model is 1793mm, ref.3).

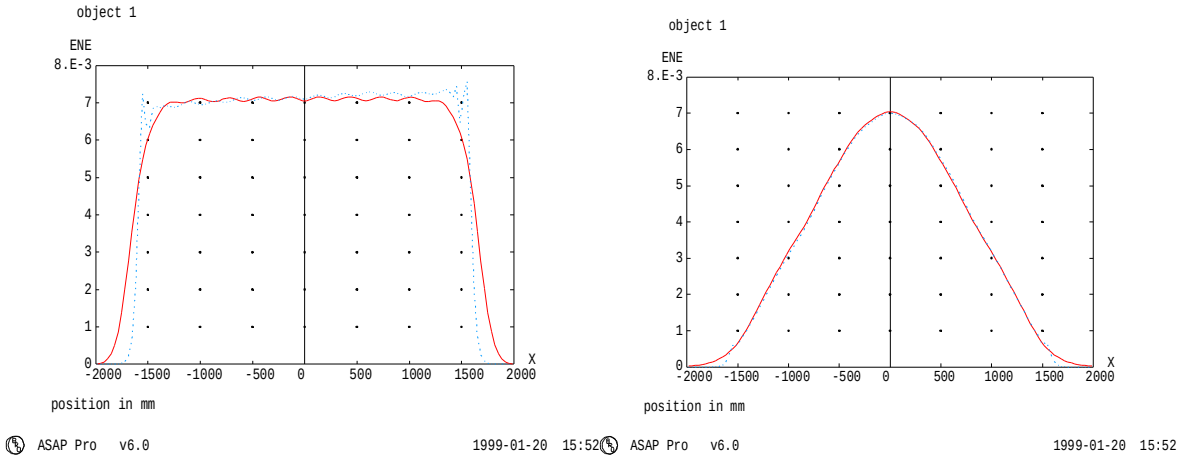

(a) (b)

Figure 3. Cross-section of beam (intensity) patterns incident on M1, solid line= without M2 clipping, dotted= with M2 clipping. (a) Top-hat case (b) Gaussian case. M1 radius is 1793mm.

Figure 4. shows the beam patterns on the sky, again for the cases with & without clipping by M2, on a log scale to show the side-lobe levels. Points to note are that in the top-hat case (a) with no clipping (solid line) the side lobes are lower than those for an Airy pattern, due to the field-stop induced blurring of the top-hat edge as described above. With the M2 clipping added (dotted line) the side lobe levels are increased, and the pattern is closer to an airy pattern. This is to be expected since the clipping restores the top-hat shape (adding edge-diffraction). In the gaussian case (b) the beam pattern with no clipping (solid line) has side lobe levels much lower than those in (a) , e.g. the first ring is more than an order of magnitude lower, as is expected as the beam is more gaussian-like. The effect of the clipping (dotted line) is again to raise the side-lobe levels, but they are still lower than those of the top-hat case, due the lower edge-taper at which clipping occurs (1/e^2 times lower).

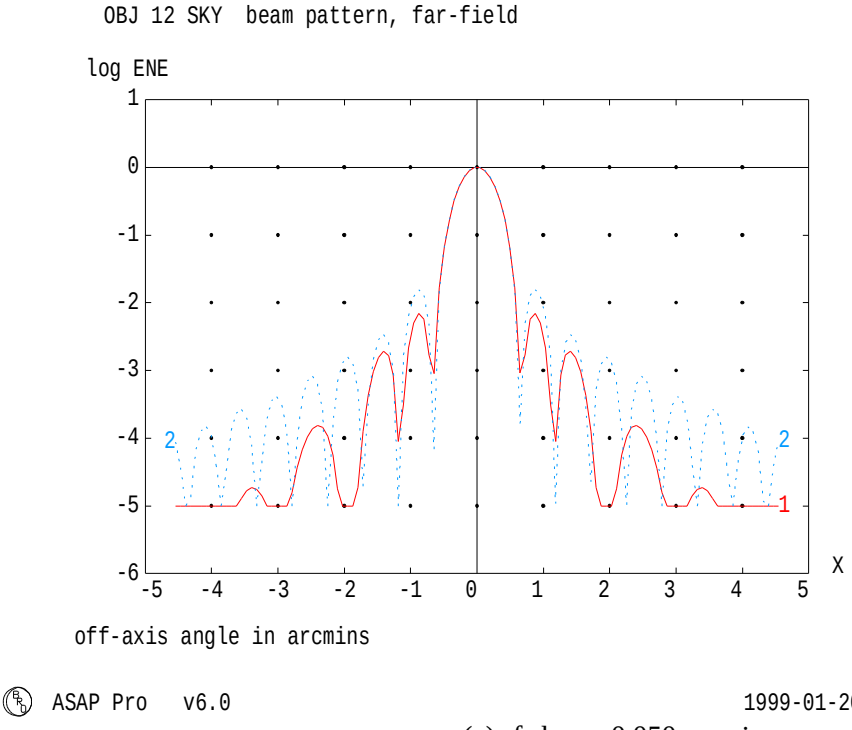

(a) fwhm = 0.050 arcmin

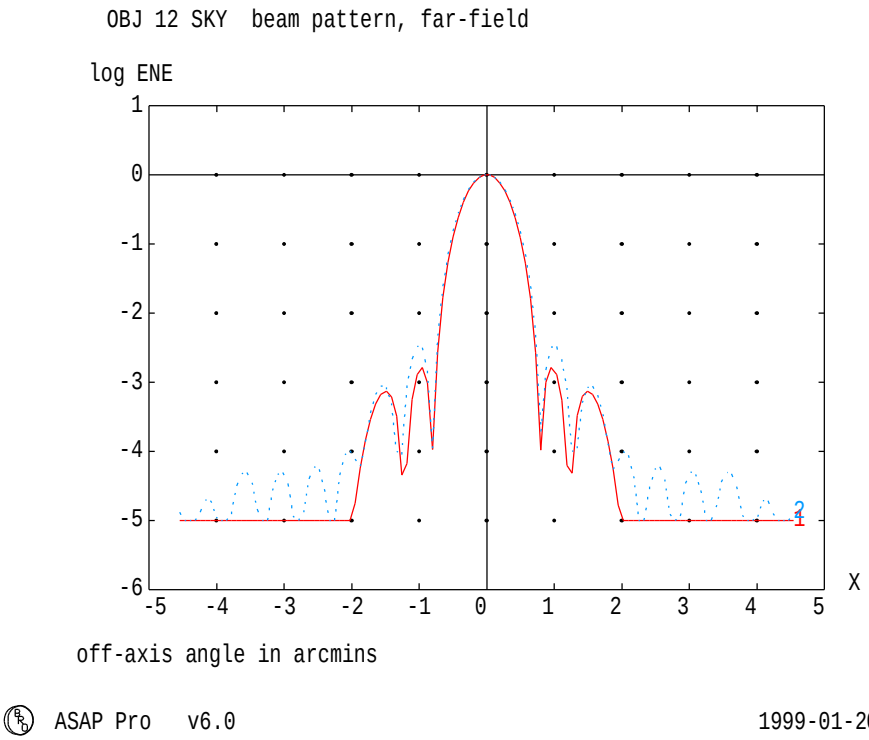

(b) fwhm = 0.057 arcmin

Figure 4. Cross-section of beam (intensity) patterns on sky, solid line= without M2 clipping, dotted= with M2 clipping. (a) Top-hat case (b) Gaussian case. Horizontal divisions are arcmins x10.

Stray-light levels.

For the components where part of the pattern lies on the surround, the detector partly sees the surround which can incorporates surfaces within the spacecraft having larger emissivity than the mirrors (viewed either directly or via further reflections) . The surround thereby contributes on-board thermal emission to the background level. Here we call this the 'clipping-background'.

The clipping background will vary with detector position in the array, increasing as we go from the centre of the array outwards, introducing increasingly severe clipping at mirror edges. The exception to this is components near pupil planes, such as M2, where the beams from each detector are co-incident, so that the clipping is similar at all positions in the field. It also varies with wavelength, becoming more severe at longer wavelengths

The clipping-background levels are expressed as a fraction η of the level due to the primary & secondary mirrors, as this is near to the level of the ideal BLIP condition. This fraction is written

$$h = \frac{e_s . P(T_s) . B_S}{2 . e_m . P(T_m).}$$

where ε: emissivity
P(T) black body Planck function.
T temperature.
B_S is the fraction of the beam flux which is on the surround surface.

And the subscripts s and m denote surround and telescope mirror emissivities respectively. The factor 2 in the denomenator is to account for the two telescope mirrors. The beam fraction B_S is equivalent to the integrated BDDF used in ref.4.

The parameters P and B_S are actually wavelength dependent, but for P this is not important since all the temperatures considered are the same ($T_S = T_M$). For B_S the wavelength-dependence requires that the analysis is repeated over the range of wavelengths, whereas here we use only λ=0.5mm as an 'average

Portion of M2 Surround	Beam fraction on surround B_s	Surround emissivity	Temp.	Background level h
Non-spider, (space viewing)	0.13	1	Cold space	**?**
Spider	0.13x 1/16	1	Telescope	**0.4**

(a) top-hat

(b)

Portion of M2 Surround	Beam fraction on surround B_s	Surround emissivity	Temp.	Background level h
Non-spider, (space viewing)	0.02	1	Cold space	**?**
Spider	0.02x 1/16	1	Telescope	**0.06**

(b) gaussian

Table 1. Stray light level from M2 surround (a) top-hat & (b) gaussian cases.

case' for this band. B_S is calculated from the beam patterns of fig.2, taking into account that the patterns are actually 2-D.

M2 surround.
For the M2 clipping the background is calculated as shown in table1. The portion of surround not hitting the spider is assumed to be transmitted to space, where it would lead to a susceptibility to long wavelength sources in a conical pattern around the line-of-sight, of half angle 3.2 degrees. The effective emissivity & temperature to use in this case are TBD & hence so is the straylight level. The portion of surround lying on the spider is estimated from the drawings in the telescope spec. ref. 5 to be 1/16 of the M2 perimeter. In ref.6 this area is allocated an emissivity $\varepsilon_s = 0.04$, but it will also reflect the beam incident on it, eventually onto other parts of the spacecraft having high emissivity (e.g. the sun-shield. Here we take as a worst case an effective $\varepsilon_s = 1$ for the eventual end of this stray-light path, and assume that the temperature there the same as that of the mirrors. As shown this gives a background level fraction from equation (2) of η=0.4 or 0.06 for top-hat or gaussian cases respectively. However, this contribution becomes unacceptable it may be blocked by placing notches in the instrument cold stops at the image of each spider leg (a Lyot stop with relatively small throughput loss).

M1 surround.
The background level due to portion of the beam lying on the sun-shield is TBD but is expected to be low in the case where M2 clipping occurs, as shown in fig.4. In addition the large beam size in this region minimises the further diffractive spreading of the beam outwards from M1. To calculate this contribution an alternative method is needed because the ASAP computation has poor accuracy at positions where the intensity is low (larger diffraction angles). This is a numerical problem also present in Fourier and Electromagnetic methods and it is overcome by the geometric theory of diffraction (GTD) methods such as those of BDDF and APART.

Conclusion.
The stray-light background levels in the case of no undersizing of SPIRE relative to the telescope, appear to be manageable. Therefore in view of the need to maximise the beam filling of the telescope aperture, it is allowable to have a minimal undersizing of the SPIRE pupil. This minimum undersizing could be that needed for geometric optics e.g. pupil aberrations and tolerances only (a few percent) , and would not

need to include the much larger undersize needed for blocking of edge-diffraction (Lyot stopping) at long wavelength (e.g. fig.2).

References.

1. "Beam patterns in PHOT-BOL and telescope" RAL/N0006.3
2. "Modelling the effect of multiple beam clipping in sub-mm instruments ISO-LWS & FIRST-SPIRE" SPIE Vol.3426 p.313
3. "Stray light analysis of PHOT". RAL/N0021.01.
4. "The level of photometric background signal from the optics" RAL/N0007
5. "FIRST Telescope spec." PT-RQ-04671
6. FIRST-L2 presentation, Chapter 4 Payload module (Daimler-Benz Aero.16-7-97)

Appendix 1.

In ASAP the beam is described by a spatial array of gaussian modes, so its edge slope is determined by the size of the outermost mode, and this in turn is set by the sample spacing Δx, plus the degree of mode overlap (default factor = 1.414). The value required to fit the beam shape to that given by (1) is then approx.

$\Delta x = (0.5.\lambda F)/1.414$